Vernier Second-order Microring Resonator for Wavelength Selective Switch

Tongxin Yang
School of Integrated Circuits
Beijing University of Posts and Telecommunications
Beijing, China
0009-0009-9757-3799

Shiqi Zhang
School of Integrated Circuits
Beijing University of Posts and Telecommunications
Beijing, China
0009-0004-0231-2769

Zilong Liu
The 54th Research Institute of China Electronic Technology Group Corporation
Shijiazhuang, China
0009-0000-5280-5546

Xiaoran Zhu
School of Science
Beijing University of Posts and Telecommunications
Beijing, China
0009-0004-3741-3009

Enge Zhang
School of Integrated Circuits
Beijing University of Posts and Telecommunications
Beijing, China
0009-0005-8207-0188

Liuwei Chen
School of Integrated Circuits
Beijing University of Posts and Telecommunications
Beijing, China
0009-0008-0804-3482

Xu Yang
The 54th Research Institute of China Electronic Technology Group Corporation
Shijiazhuang, China
yangxumail@foxmail.com

Lei Zhang
School of Integrated Circuits
Beijing University of Posts and Telecommunications
Beijing, China
zhang-lei@bupt.edu.cn

***Abstract*—We present a wavelength selective switch (WSS) that is based on two Vernier 2nd-order microring resonators (MRRs). Each 2nd-order MRR has two racetrack cavities with perimeters of 78.8 μm and 105.2 μm, respectively, producing a free spectral range around 22 nm. The WSS exhibits a 3dB bandwidth of 85 GHz and an extinction ratio around 10 dB.**

Keywords—High-order Microring Resonator, Vernier effect, Wavelength selective switch.

I. INTRODUCTION

Wavelength division multiplexing (WDM) is a widely used technology in long-haul fiber communication networks and data centers to accommodate the continuously increasing amount of data traffic [1-3]. At the network nodes, optical switches are required to route different optical signals to different destinations. The Mach-Zehnder interferometer (MZI) optical switch is one of the two main types of optical switches, the other being the microring resonator (MRR) optical switch [4-10]. The MZI optical switch with balanced interference arms can act as a broadband switch. In other words, the MZI optical switch handles a range of wavelengths together. On the contrary, the MRR optical switch is wavelength selective and can switch different wavelengths to different ports. Moreover, the MRR optical switch is preferred due to its small size and low power consumption. However, the shortcomings of a MRR with a single ring cavity are that it has a Lorentzian response inducing signal distortion and usually a narrow free spectral range (FSR) which limits the channel numbers it can accommodate.

To modify the response spectrum and enhance the FSR, we propose a wavelength selective switch (WSS) based on Vernier second-order microring resonator. The WSS is composed of two cascaded racetrack cavities with different perimeters. We cascade two such Vernier second-order MRRs to make a 2-channel WSS, with each second-order MRR handling one wavelength. We fabricate the chip using electron beam lithography and characterize the device with broadband source. The measurement results show that the proposed Vernier second-order MRR has a flat-top spectral response and an enhanced FSR around 22 nm.

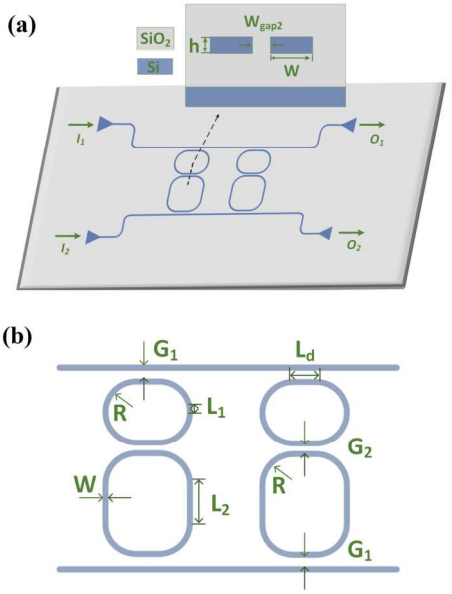

Fig. 1. (a) Schematic of the proposed wavelength selective switch and the cross section of the coupling region. (b) Design parameter of the WSS.

II. DESIGN

Figure 1 (a) shows the proposed 2-ch WSS consisting of two stages of second-order MRRs, each handling one specific wavelength. To utilize the Vernier effect in one second-order MRR, we employ two racetrack cavities with different perimeters. The FSRs of the two racetrack cavities are given by the following formula,

$$FSR_i = \frac{\lambda_0^2}{n_g \cdot (2\pi R + 2L_d + 2L_i)}, \ i = 1, 2 \qquad (1)$$

The parameter n_g in formula (1) is the average group refractive index of the waveguides constituting the racetrack. The λ_0 is operating wavelength in vacuum. L_d is the length of straight waveguide in the coupling regions. L_1 and L_2 are lengths of the other two straight segments in each racetrack,

whose function is to tune the cavity perimeter. The FSR of the cascaded structure, i.e. the second-order MRR is,

$$FSR = \frac{FSR_1 \cdot FSR_2}{|FSR_1 - FSR_2|} \quad (2)$$

where FSR_1 and FSR_2 are the FSRs of the two racetrack cavities, respectively.

According to Eq. 2, we can deduce that the closer the amplitudes of FSR_1 and FSR_2 are, the larger the overall FSR of the second-order MRR is. However, it is not recommended to use two cavities with perimeters that are too close to each other. This is because each cavity has its own spectral response with finite bandwidth. Two cavities with too close FSRs will deteriorate the Vernier effect.

The channel waveguide constituting the device has a width of 500 nm and a height of 220 nm. We chose the L_D to be 8 μm. Such a coupling length will result in electric-field cross-coupling ratios of 0.5 and 0.15 for bus-ring and ring-ring coupling, respectively, with a gap spacing of 186 nm and 324 nm. We chose these parameters to make it compatible with further implementation in 0.18μm photolithography. Additionally, the combination of cross-coupling ratios of 0.5 and 0.15 will produce a flat-top response of the second-order MRR [11].

In the small and large racetracks in Fig. 1(b), we chose the L_1 and L_2 to be 0 and 13.2 μm. The circular waveguides connecting these straight ones have a radius of 10 μm. Thus, the two racetrack cavities have perimeters of about 78.8 μm and 105.2 μm, respectively. The FSR_1 and FSR_2 are around 7.6 nm and 5.7 nm, respectively, if we assume the average group refractive index to be 4.0 in both racetrack cavities. Using Eq. (2), we can deduce that the overall FSR of the second-order MRR is about 22.8 nm.

The parameters of the two second-order MRRs are identical, thus they have the same resonance wavelengths as well as the line shapes. To make them operate at two different wavelengths, we need to rely on some tuning mechanisms to shift the resonance wavelengths of the two MRRs independently. In our design, we use four resistance heaters to tune the four cavities in Fig. 1. Suppose two continuous waves with different wavelengths λ_1 and λ_2 input at port I_1, which will be routed by the 1st and 2nd second-order MRRs, respectively.

III. Fabrication and Experimental Results

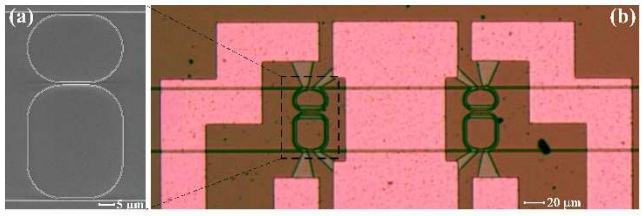

Fig. 2. (a) SEM image of one second-order microring resonators. (b) Microscope image of the fabricated 2-ch wavelength selective switch.

The device is fabricated using electron-beam lithography. Figure 2 (a) shows the scanning electron microscope (SEM) image of one second-order MRR. Figure 2 (b) shows the optical microscope picture of the 2-ch wavelength selective switch with an effective footprint of about 0.25×0.45 mm^2, including the electrical pads. The coupling of the fiber to the chip is accomplished using broadband grating couplers (GC). The experimental spectra shown below are normalized with a straight waveguide with GC at both ends.

TABLE I. The States of the Two MRRs and the Routing Results

State	*MRR 1*	*MRR 2*	*Routing function*
00	Off-resonance	Off-resonance	Both signals go to port O_1
01	Off-resonance	On-resonance	λ_1 goes to port O_1, λ_2 goes to port O_2
10	On-resonance	Off-resonance	λ_1 goes to port O_2, λ_2 goes to port O_1
11	On-resonance	On-resonance	Both signals go to port O_2

As shown in Table 1, we use two digits '1' and '0' to indicate that one second-order MRR is on-resonance and off-resonance, respectively. A combination of two digits is used to illustrate the states of the two second-order MRRs. For example, '11' means that the 1st and 2nd MRRs are on-resonance at λ_1 and λ_2, respectively. Table 1 use the same port definition as in Fig. 1.

Figure 3 shows the normalized spectra of two stages of second-order MRRs under three different working states. The two dotted lines indicates the two virtual working wavelengths λ_1 and λ_2. In all the measurements, light launched into port I_1. Figures 3 (a) and (b) exhibit the transmission spectra of the drop port (O_2) and through port (O_1), respectively, under the state '00'. Both λ_1 and λ_2 are routed to O_1 with minimal on-chip loss. The extinction ratio (ER) beyond 20 dB in Fig. 3 (a) means that less than 1% of the input power at λ_1 and λ_2 leaks to port O_2.

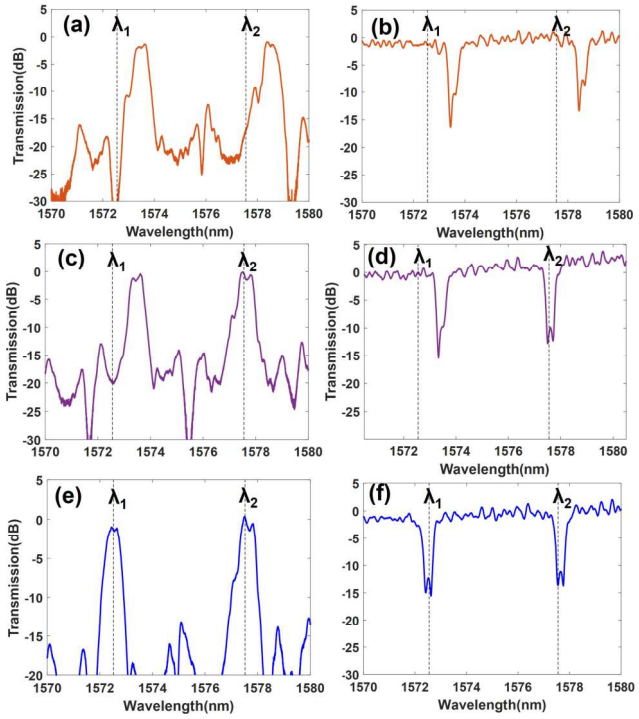

Fig. 3. The experimental result of the cascaded WSS. The normalized spectra of two stages MRRs at state of (a) O_2 port "00", (b) O_1 port "00", (c) O_2 port "01", (d) O_1 port "01", (e) O_2 port "11", (f) O_1 port "11".

Figures 3 (c) and (d) show the normalized spectra under the state '01'. The input from port I_1 at wavelength λ_1 is routed to O_1, with around 1% power leaked to port O_2 (i.e. the crosstalk is around -20dB). The input from port I_1 at wavelength λ_2 is routed to O_2, with around 10% power leaked to port O_1 (i.e. the crosstalk is around -10dB).

The normalized spectra under the state '11' are shown in Figures 3 (e) and (f). Both λ_1 and λ_2 are routed to port O_2, as

shown in Fig. 3(e). Fig. 3(f) shows that less than 10% of the input powers at λ_1 and λ_2 leak to port O_1.

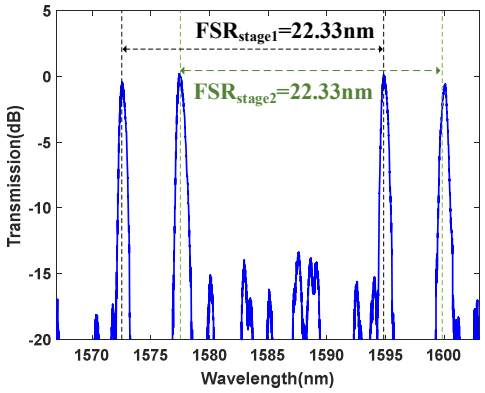

Fig. 4. Normalized spectra of the 2-ch WSS showing the entire FSR.

Figure 4 shows the spectrum of the device in a broad range. The measured FSR of each 2nd-order MRR is about 22.33nm, which agrees well with the prediction given by Eq. 2. The 3dB bandwidth of the passband is about 85GHz, which is sufficient for the undistorted transmission of analog or digital signals currently used in data centers or microwave photonic systems.

IV. Conclusion

In summary, we have proposed a wavelength selective switch using two Vernier second-order microring resonators. Each second-order MRR has two racetrack cavities with perimeters of 78.8 μm and 105.2 μm, respectively, producing a free spectral range around 22 nm. The WSS exhibits a 3dB bandwidth of 85 GHz and an extinction ratio around 10 dB.

Acknowledgment

This project is supported by National Natural Science Foundation of China (Grant No. 61975198), the Fund of State Key Laboratory of Information Photonics and Optical Communications (IPOC2021ZT11).

References

[1] S. Wei, T. Ye, G. Antoine, "Scaling capacity of fiber-optic transmission systems via silicon photonics," Nanophotonics, vol. 9, no. 16, pp. 4629-4663, 2020.

[2] A. Khope, S. Liu, Z. Zhang, A. Netherthon, J. Bowers, "2 λ switch," Optics Letters, 2020.

[3] J. He, J. Yang, H. Ma, X. Jiang, H. Yuan, Y. Yu, "Design of a Multi-Functional Integrated Optical Switch Based on Phase Change Materials," Photonics, vol.9, no.5, pp.320, 2022.

[4] A. S. P. Khope, M. Saeidi, R. Yu, X. Wu, A. M. Netherton, Yuan Liu, Z. Zhang, Y. Xia, G. Fleeman, A. Spott, S. Pinna, C. Schow, R. Helkey, L. Theogarajan, R. C. Alferness, A. A. M. Saleh, J. E. Bowers, "Multi-wavelength selective crossbar switch," Opt. Express pp. 5203-5216, 2019.

[5] A. S. P. Khope, R. Helkey, S. Liu, S. Khope, R. C. Alferness, A. A. M. Saleh, J. E. Bowers, "Scalable multicast hybrid broadband-crossbar wavelength selective switch: proposal and analysis," Opt. Lett. pp. 448-451, 2021.

[6] T. Kita and M. Mendez-Astudillo, "Ultrafast Silicon MZI Optical Switch With Periodic Electrodes and Integrated Heat Sink," in Journal of Lightwave Technology, vol. 39, no. 15, pp. 5054-5060, 2021.

[7] K. Ikeda, K. Suzuki, R. Konoike, S. Namiki and H. Kawashima, "Progress and Future Prospect of Silicon Photonics Based Large Scale Optical Switches," OptoElectronics and Communications Conference (OECC), pp. 1-3, 2022.

[8] T. Kita and M. Mendez-Astudillo, "Ultrafast Silicon MZI Optical Switch With Periodic Electrodes and Integrated Heat Sink," in Journal of Lightwave Technology, vol. 39, no. 15, pp. 5054-5060, Aug.1, 2021.

[9] A. Khope, R. Helkey, S. Liu, " A Scalable Multicast Hybrid Broadband Crossbar Wavelength Selective Switch For Datacenters", IEEE 11th Annual Computing and Communication Workshop and Conference (CCWC), 2021.

[10] X. Chen, J. Lin, K. Wang, "A Review of Silicon - Based Integrated Optical Switches", Laser & Photonics Reviews, pp. 2200571, 2023.

[11] L. Zhang, H. Zhao, H. Wang, S. Shao, W. Tian, J. Ding, X. Fu, L. Yang, "Cascading Second-Order Microring Resonators for a Box-Like Filter Response," J. Lightwave Technol, vol. 35, pp. 5347-5360, 2017.